PHYSICS AND CHEMISTRY OF SOLID STATE
V. 22, No. 4 (2021) pp. 607-613
Section: Physics

DOI: 10.15330/pcss.22.4.607-613

Vasyl Stefanyk Precarpathian National University

ФІЗИКА І ХІМІЯ ТВЕРДОГО ТІЛА
Т. 22, № 4 (2021) С. 607-613
Фізико-математичні науки

PACS: 77.84.Lf ISSN 1729-4428

Asif Ali, Hina Zahid

Dielectric, Ferroelectric and Optical Properties of Na and Nb co-Doped $(Bi_{0.5}Na_{0.5})_{0.94}Ba_{0.06}TiO_3$

Department of Physics, Abdul Wali Khan University Mardan, Pakistan, asif.lfmd@gmail.com

$[(Bi_{0.5}Na_{0.5})_{0.94}Ba_{0.06}]_{1-x}Na_xTi_{1-x}Nb_xO_3$ (x = 0.05 and 0.10) ceramics were prepared via conventional solid-state sintering route. X-ray diffraction analysis of the samples exhibited the formation of the cubic structure. Similar structure was observed from the Raman spectra of the samples. The optical band gap of the samples slightly decreased from 3.08 to 3.06 eV with increasing level of Na^+ and Nb^{5+}. The addition of Na^+ and Nb^{5+} shifted T_m towards room temperature (RT). The sample x = 0.05 had a stable relative permittivity $\varepsilon_{r(mid)}$ = 3914 across the temperature range 79 - 350 °C and tanδ < 0.025 (104 - 279 °C). The energy density of sample with x = 0.05 was 0.4 J/cm^3 which decreased to 0.32 J/cm^3 at an applied electric field of 50 kV/cm with further substitution of Na^+ and Nb^{5+} (i.e., x = 0.10).

Keywords: $BaTiO_3$; $Bi_{0.5}Na_{0.5}TiO_3$; dielectric properties; ferroelectric properties; energy density.

Received 1 Juiy 2021; Accepted 15 September 2021.

Introduction

Dielectric materials are extensively used in different electronic applications in the form of capacitors, resistors, nonlinear dielectric thin films, advanced pulsed capacitors etc. [1-3]. Capacitor is an important electronic component because it is mounted on almost every electronic circuit. Capacitor could store electric charge therefore, in the previous years, researchers have investigated numerous materials for high energy-storage applications. Among these materials, lead-based material possess high energy-storage such as $Pb(Nb_{2/3}Mg_{1/3})O_3$ (PNM), $Pb(Nb_{2/3}Zn_{1/3})O_3$ (PNZ) [4]. The lead based film based on 0.426PNZ-0.308PNM-0.23$PbTiO_3$ is reported to have a high-energy density of 15.8 J/cm^3 under an applied E = 700 kV/cm [5]. Similarly, other lead based compositions have also high energy-density up to 65 J/cm^3, which was obtained for $(Pb_{0.92}La_{0.08})Zr_{0.52}Ti_{0.48})O_3$ thin film when deposited on the substrate using lanthanum as an intermediate layer [6]. Due to the toxic nature of lead, which is dangerous to human-health and environment, lead-free dielectrics are always preferred for practical applications. According to the directives by European Union, that lead-based materials should not be used as a base substance. In comparison, $Bi_{0.5}Na_{0.5}TiO_3$ (BNT) and $BaTiO_3$ (BT) based materials, which have some unique characteristics because of its crystal structure, dielectric, ferroelectric and piezoelectric properties, and therefore, remain a good choice for industrial applications. Although, they have their own limitations as well, but researchers have reported their solid solutions with other materials to get an optimum set of properties for specific applications [7-10].

Among the solid solutions, $(1-x)Bi_{0.5}Na_{0.5}TiO_3$-$xBaTiO_3$ (BNT-BT) system is of great interest [11] because at the morphotropic phase boundary (MPB), a high relative permittivity was observed in comparison to both end members. MPB displays a coexisting or transition region where mostly a pseudocubic structure is formed. BNT and BT both are ferroelectric compounds with complex crystallographic structures and have interesting ferroelectric properties. BNT has high Curie temperature 'T_c' of about 320 °C, whereas BT has a very small 'T_c'. Their resulting solid solution shows high and stable permittivity, low conduction losses or dielectric losses under a very high temperature range [12]. Temperature dependent electrical

properties of lead-free $0.94(Bi_{0.5}Na_{0.5}TiO_3)$-$0.06BaTiO_3$ ceramics have been investigated [13]. At temperature below 100 °C, a transition from rhombohedral to tetragonal phase shows dominant FE order and as temperature reaches to 100 °C, the antiferroelectric (AFE) order prevails. The composition shows a giant unipolar and bipolar strain near the phase transition among FE to AFE. In BNT-BT system, MPB has been observed for 94 mol % BNT and 6 mol. % BT i.e. $(Bi_{0.5}Na_{0.5})_{0.94}Ba_{0.06}TiO_3$ when synthesized by aerosol deposition method (ADM) at room temperature (RT) [14]. In another study, $(Bi_{0.5}Na_{0.5})_{0.94}Ba_{0.06}TiO_3$ with different ratios of Na and Bi were reported to exhibit a high remnant polarization of 28.8 to 40.4 μC/cm^2 [15]. Similarly, the effect of the La^{3+} and Zr^{4+} co-doping were observed to enhance the energy storage properties of the La^{3+} and Zr^{4+} doped $(Bi_{0.5}Na_{0.5})_{0.93}Ba_{0.07}TiO_3$ solid solution prepared by the conventional solid-state reaction route [16]. Their substitution reduced P_r and the E_c but enhanced the energy storage of the ceramics. The optimal energy storage density of 1.21 J/cm^3 were obtain at 100 kV/cm. The efficiency of the ceramics was increased up to 77 %. Similarly, an energy storage density of 0.59 J/cm^3 was reported for $(Bi_{0.5}Na_{0.5})_{0.94}Ba_{0.06}TiO_3$-$Ka_{0.5}Na_{0.5}NbO_3$ ceramics at E = 56 kV/cm [17]. The energy storage properties of the $(1\text{-}x)(0.92Bi_{0.5}Na_{0.5}TiO_3–0.08BaTiO_3)–xNa_{0.73}Bi_{0.09}NbO_3$ ceramics were investigated [18]. Optimum properties were obtained for the composition x = 0.20 which exhibited J_{rec} = 1.36 J/cm^3 and η = 74 %. Similarly, there are so many other $NaNbO_3$–modified systems that have been investigated for capacitors applications which shows the shifting of Curie point towards RT and below, and also resulted into increase the thermal stability of dielectrics [19, 20]. Therefore, keeping in view the above discussion, we have chosen $[(Bi_{0.5}Na_{0.5})_{0.94}Ba_{0.06}]_{1-x}Na_xTi_{1-x}Nb_xO_3$ system and investigated dielectric, ferroelectric and optical properties for potential application in electronic industry.

I. Experimental technique

$[(Bi_{0.5}Na_{0.5})_{0.94}Ba_{0.06}]_{1-x}Na_xTi_{1-x}Nb_xO_3$ (x = 0.05 and 0.10) ceramics were prepared using reagent grade $BaCO_3$, Na_2CO_3, TiO_2, Bi_2O_3 and Nb_2O_5. The raw powders were dried and then weighed according to the molar ratios. The batch compositions were mixed and milled using mortar and pestles in acetone. The milling was continued for an hour for homogeneous mixing. The mixed/milled powders were dried in oven. The powders were kept in closed alumina crucibles and calcined at 900 °C for 2 h. To dissociate agglomerations (if any) and reduce particle size, the calcined powders were re-milled. The calcined powders were pressed into circular pellets of 10 mm diameter by pressing them at a pressure of about 1/2 ton for 60 sec, using a uniaxial hydraulic pellet press. The green pellets were sintered at temperature ranging from 1100 to 1150 °C for 2 h.

Phase identification of the sintered pellets was carried out using a Philips X- ray diffractometer with Cu-Kα radiation source, having wavelength of 1.5406 Å was used. Raman spectra were collected at room temperature using Renishaw-Raman spectrometer using 514 nm of Ar laser. Microstructure of the samples was examined using a JEOL-Scanning Electron Microscopy (SEM). Dielectric properties as a function of temperature were measured using HP-4284A LCR meter. The polarization–electric field (P–E) hysteresis loops were measured using Radiant Ferroelectric tester at room temperature.

II. Results and discussion

X-ray diffraction patterns of the $[(Bi_{0.5}Na_{0.5})_{0.94}Ba_{0.06}]_{1-x}Na_xTi_{1-x}Nb_xO_3$ (x = 0.05 and 0.10) samples, sintered at 1150 °C for 2 h are shown in Fig. 1.

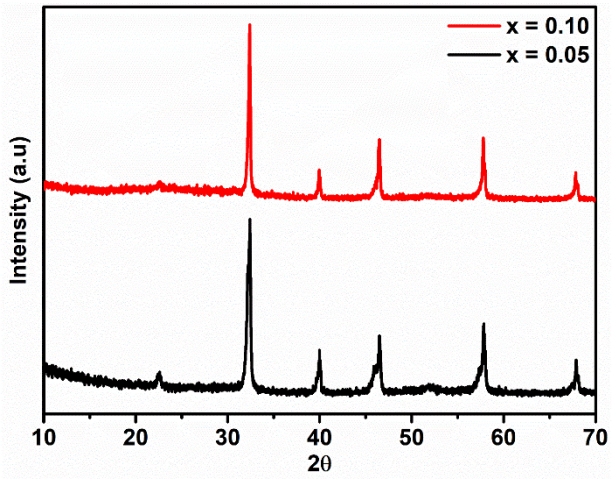

Fig. 1. X-ray diffraction pattern of $[(Bi_{0.5}Na_{0.5})_{0.94}Ba_{0.06}]_{1-x}Na_xTi_{1-x}Nb_xO_3$ (x = 0.05 and 0.10), sintered 1150 °C for 2 h, showing the formation of single-phase perovskite structure.

The diffraction patterns matched JCPDS # 89-3109, for cubic structure. No evidence of secondary phase(s) was found in the diffraction patterns of these samples which shows the solubility of the Na^+ and Nb^{5+} in the base composition BNBT. From the X-ray diffraction patterns, it can be observed that the peak ~ 46.5° has been splitted and has become a single peak with the high concentration of sodium niobate (NN). For the composition at x = 0.05, the splitting of (002)/(200) is also reported previously [21]. This also shows the character of morphtrophic phase boundries of BNT-NN. The merging of peaks can be explained on the basis of incorporation of Na^+ and Nb^{5+} in BNBT. Since, Nb^{5+} is incorporated at the B-Site having an ion radius of 0.64 Å and has a different valency and ionic radius than the Ti^{4+} [22]. Thus, we conclude that at x = 0.05, the structure is psudocubic and at x = 0.10, the structure transform to a cubic structure.

Raman spectra of the $[(Bi_{0.5}Na_{0.5})_{0.94}Ba_{0.06}]_{1-x}Na_xTi_{1-x}Nb_xO_3$ (x = 0.05, 0.10) samples are shown in Figure 2. The Raman spectra is similar to that of previously reported for the BNT-NN [23]. The peak near ~114 cm^{-1} is assigned as a A1(TO_1) mode which is due to the vibration of A–site cations [24]. The band near ~261 cm^{-1} is dominated by Ti-O vibration

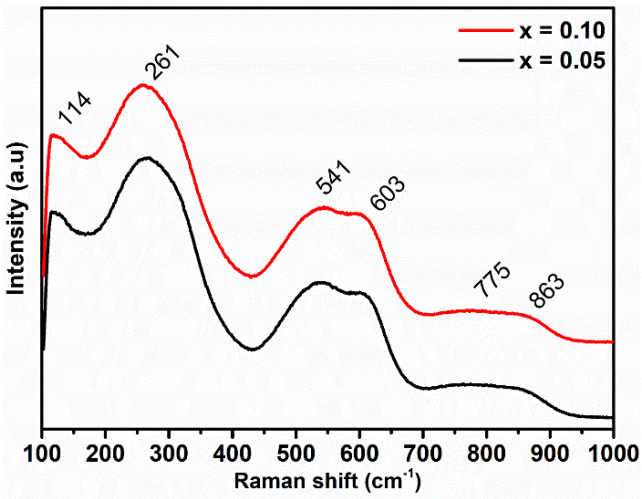

Fig. 2. Raman spectrum of $[(Bi_{0.5}Na_{0.5})_{0.94}Ba_{0.06}]_{1-x}Na_xTi_{1-x}Nb_xO_3$ (x = 0.05 and 0.10), sintered 1150 °C for 2 h.

are assigned as $E(TO_2)$. The bands near 261 and 603 cm^{-1} were observed to shift to lower wavenumbers with increasing concentration of the NN which may be due to incorporation of Nb^{5+}, forming an NbO_6 octahedra and increasing concentration of Na^+ ions [23]. The band at ~541 cm^{-1} and 603 cm^{-1} may be due different sets of TiO_6 by NbO_6 octahedra [25]. The broader peak at 775 cm^{-1} is observed to be the same for all sample which are assigned as (A_1g) appear only when the B-Site is shared by two are more cation [26]. The first sharp Raman band and the weaker broader which is indicative polar nano regions (PNRs) [27]. The Raman spectroscopy results were in good agreement with the XRD result which confirm the formation of the cubic/pseudocubic structure. The Raman bands of $[(Bi_{0.5}Na_{0.5})_{0.94}Ba_{0.06}]_{1-x}Na_xTi_{1-x}Nb_xO_3$ (x = 0.05, 0.10) are compared and in good agreement with the literature, Table 1.

Figure 3 shows the SEM micrographs of the polished surface and thermally etched at temperature 10 % less

Table 1

Comparison of the Raman band of $[(Bi_{0.5}Na_{0.5})_{0.94}Ba_{0.06}]_{1-x}Na_xTi_{1-x}Nb_xO_3$ with the literature review

Composition	Raman bands						Ref.
$[(Bi_{0.5}Na_{0.5})_{0.94}Ba_{0.06}]_{1-x}Na_xTi_{1-x}Nb_xO_3$ (x = 0.05)	114	261	541	603	775	863	Present work
NBT-BT	142	281	531	585	748	860	[29]
NBT	120	274	527	573	750	869	[24]
NBT	131	279	521	576	754	829	[30]
NBT	135	276	514	582	767	845	[31]

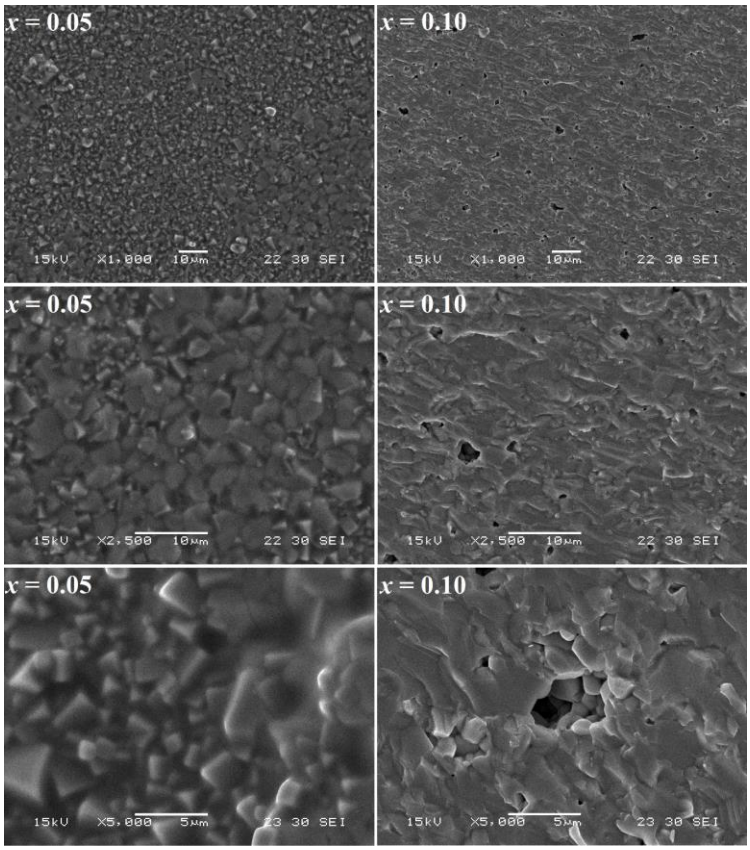

Fig. 3. SEM micrographs of the ceramic of $[(Bi_{0.5}Na_{0.5})_{0.94}Ba_{0.06}]_{1-x}Na_xTi_{1-x}Nb_xO_3$ (x = 0.05 and 0.10).

than the sintering temperature at different magnifications. The secondary electron images show polycrystalline microstructure having almost cuboidal like grains with dimensions ranging from ~1 to ~5 μm in length for the sample x = 0.05. The grains are closely bound but there were still some voids present in the microstructure with the increasing composition of the NN. No clear grain morphology was observed in the polished x = 0.10 sample; however, some cuboidal like grains can be seen in void.

Figure 4 shows the relative permittivity (ε_r) and tangent loss (tanδ) as a function of temperature at different frequencies 1 kHz to 1 MHz in the temperature - range from 25 ℃ to 500 ℃. For x = 0.05 sample, relative permittivity (3920) at temperature of maximum relative permittivity (T_m) at 252 ℃ decreased from ~2640 (at 94 ℃) with increase in x which was less than that of pure BNT-BT. Similarly a decreasing trends was observed in the $\varepsilon_{r(max)}$ at T_m which is due to replacement the Bi^{3+} having larger ionic polarizability than Na^+ [28]. The composition x = 0.05 has a maximum ε_r of 3920 with the low tanδ at RT i.e., < 0.025 at 1 KHz. The ceramic had a high ε_r value $\varepsilon_{r(mid)250}$ = 3914 ± 15 %, stable across a wide-temperature-range 79 – 350 ℃ with a minimum tanδ < 0.025 stable over the temperature-range of 104 – 279 ℃.

Further increasing the amount of NN to x = 0.10, the ceramic had a high value of relative permittivity at mid temperature i.e., ε_r = 2643 ± 15 % (45 - 374 ℃) which showed that the lower and upper temperature stability range was improved. Further the system had low tangent loss < 0.025 across 94 – 301 ℃ and minimum $\tan\delta_{(RT)}$ = 0.05 as shown in Table 2.

The energy storage properties of the dielectric material were calculated from the hysteresis loop. The polarization versus electrical field at RT is shown in the

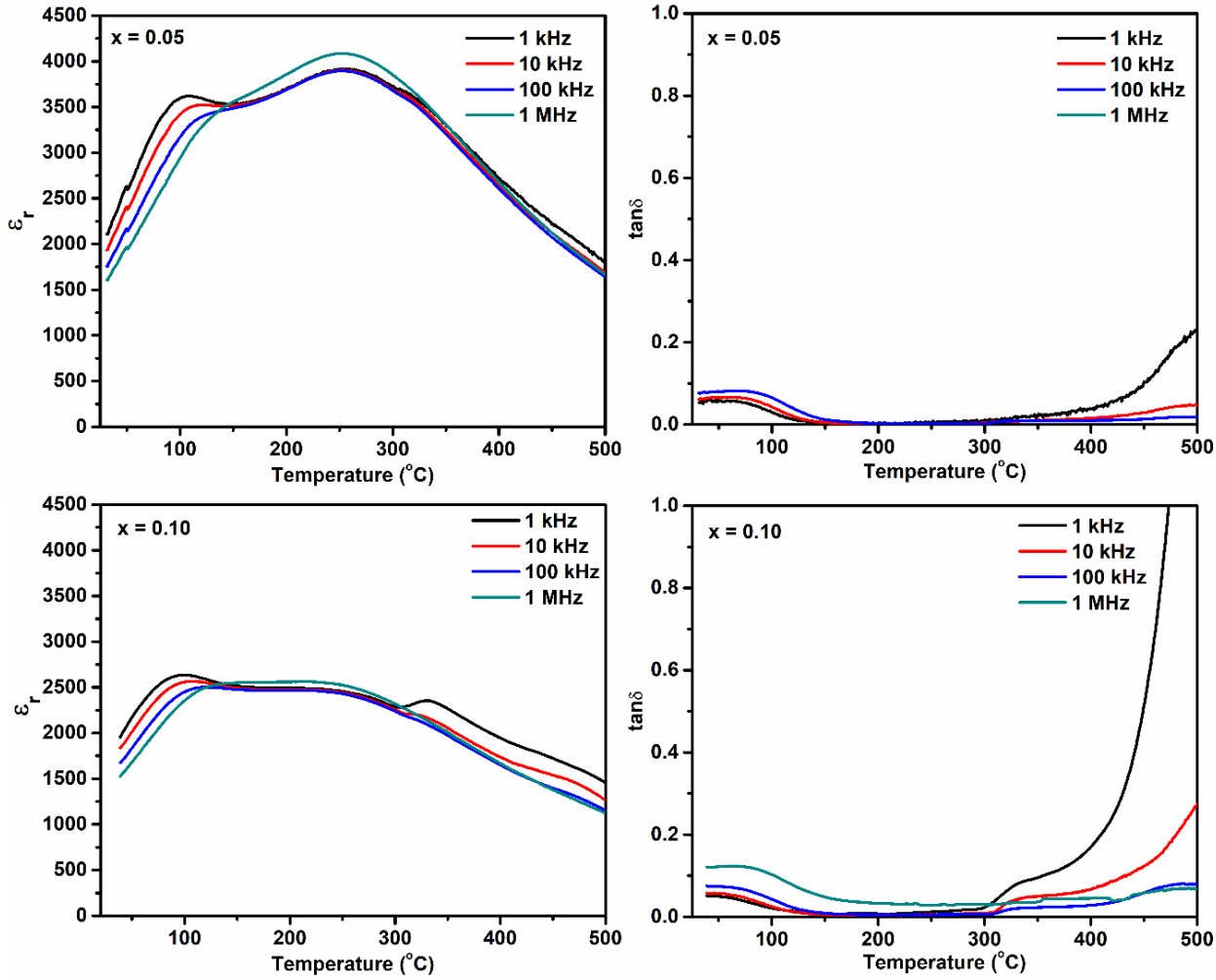

Fig. 4. Temperature versus ε_r and tanδ for $[(Bi_{0.5}Na_{0.5})_{0.94}Ba_{0.06}]_{1-x}Na_xTi_{1-x}Nb_xO_3$ (x = 0.05 and 0.10) ceramics.

Table 2

Dielectric properties of $[(Bi_{0.5}Na_{0.5})_{0.94}Ba_{0.06}]_{1-x}Na_xTi_{1-x}Nb_xO_3$ (x = 0.05, 0.10).

x	T_m (°C)	$\varepsilon_{r(max)}$	ε_r (RT)	tanδ (RT)	$\varepsilon_{r(mid)250℃}$	T−range (°C) ε_r ±15 % (1 kHz)	T-range tanδ < 0.025 (1 kHz)
0.05	252	3921	2097	0.052	3914	79-350	104−279
0.10	94	2643	1957	0.05	2566	45-374	94-301

Figure 5. The ceramics showed that the solid solution can withstand at high voltage. Maximum polarization (P_{max}) value was observed to be increase with increasing the voltage for both samples with x = 0.05 and 0.10 while the value of P_{max} was observed to be decrease with increasing concentration of x. A similar trend as observed for the relative permittivity in the upper section. For x = 0.05, the ceramics had an ED and η = 0.40 and 82 %, respectively at 50 kV, Table 3.

Table 3

P_{max}, Remnent polarization (P_r), electric field (E_c), recoverable energy (W_{res}) and efficiently (η) for $[(Bi_{0.5}Na_{0.5})_{0.94}Ba_{0.06}]_{1-x}Na_xTi_{1-x}Nb_xO_3$ (x = 0.05, 0.10) ceramics.

Compo -sition	P_{max} $(\mu C/cm^{-2})$	P_r $(\mu C/cm^2)$	E_c (kV/ cm)	W_{rec} (J/cm^3)	η %
0.05	24.35	4.08	6.95	0.40	82
0.10	16.16	1.61	4.40	0.32	72

While for x = 0.10, the system exhibited an ED and η value of 0.32 and 72 %, respectively at 50 kV. Thus, it was concluded that further introducing Na and Nb ions will degrade the efficiency and ED of the system.

In term of the direct and indirect band gap material may be characterized using UV-vis spectroscopy. Kulbelka Munk relation is used for optical absorbance, given by equation as:

$$F(R) = \frac{(1-R)^2}{2R} = \frac{\alpha}{s} \rightarrow \quad (1)$$

The absorption coefficient 'α' is directly related to F(R), optical absorbance while in the equation 's' is the scattering coefficient and 'R' is the relative reflectance. The Tauc equation is used for the band gap, given as:

$$(F(R).h\upsilon)^{\frac{1}{2}} = B(E_g - h\upsilon) \rightarrow \quad (2)$$

Figure 6 shows the plots between $(\alpha h\upsilon)^2$ versus hυ for $[(Bi_{0.5}Na_{0.5})_{0.94}Ba_{0.06}]_{1-x}Na_xTi_{1-x}Nb_xO_3$ (x = 0.05, 0.10) ceramics. The band gap calculated from these plots were 3.08 eV for sample with x = 0.05 which decreased to 3.06 eV with further increase in x up to 0.10. The substitution of Na Nb has modified the band gap values. Band gap is also influenced by oxygen vacancies but in the present case, the change is due to modification in lattice via Na and Nb doping.

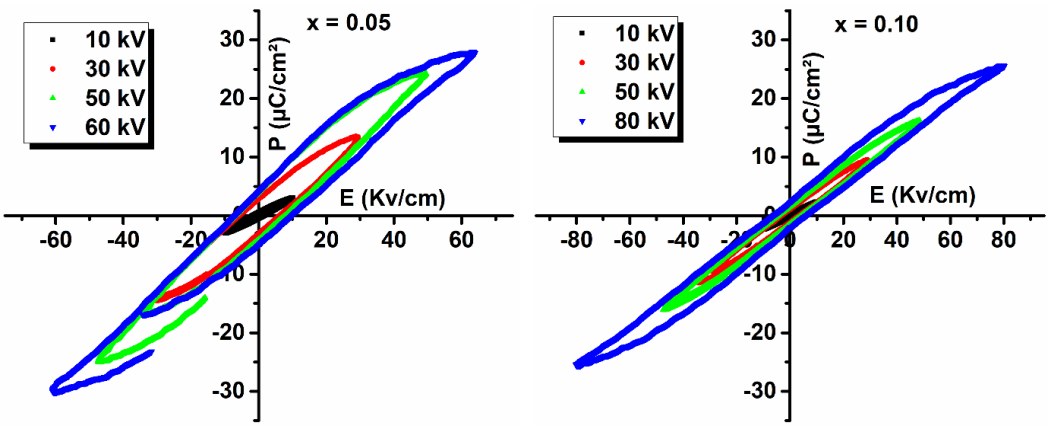

Fig. 5. PE-hysteresis Loop of $[(Bi_{0.5}Na_{0.5})_{0.94}Ba_{0.06}]_{1-x}Na_xTi_{1-x}Nb_xO_3$ (x = 0.05 and 0.10) samples measured at RT.

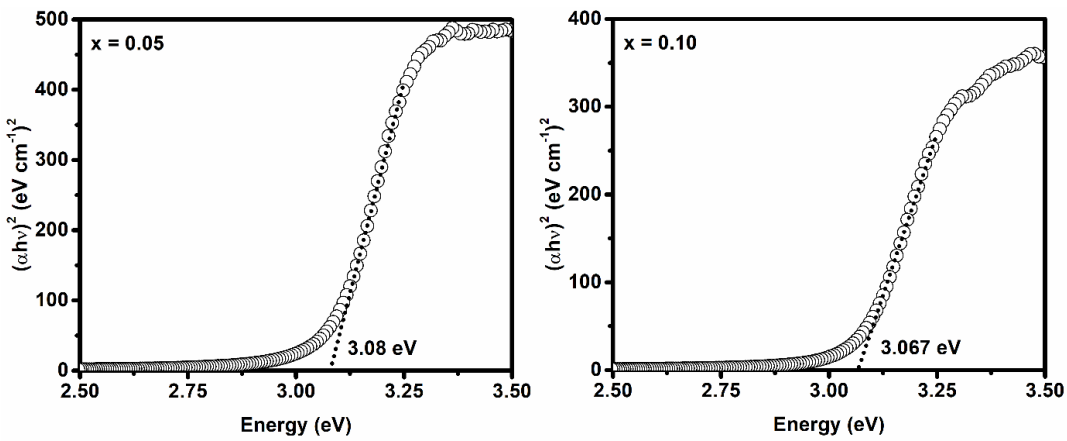

Fig. 6. Plots between $(\alpha h\upsilon)^2$ versus hυ for $[(Bi_{0.5}Na_{0.5})_{0.94}Ba_{0.06}]_{1-x}Na_xTi_{1-x}Nb_xO_3$ (x = 0.05 and 0.10) ceramics.

Conclusion

The effect of Na^+ and Nb^{5+} substitution on the structure, microstructure, dielectric properties and energy storage performance of $(Bi_{0.5}Na_{0.5})_{0.94}Ba_{0.06}TiO_3$ was investigated. X-ray diffraction analysis revealed the formation of single-phase cubic structure which was also confirmed from the Raman spectra of the ceramics. The optical band gap values were 3.08 and 3.07 eV for sample with x = 0.05 and 0.10, respectively. The dielectric properties of the ceramic solid solution were greatly affected by the addition of Na^+ and Nb^{5+}. T_m value shifted towards the low temperature from 252 °C to 94 °C with increase in *x*. The maximum dielectric constant was observed for the composition with *x* = 0.05 i.e., 3921, which was stable across the temperature range 79 – 350 °C with tanδ < 0.025 (104 - 279 °C). The temperature stability range of relative permittivity was enhanced with increase in *x* at the cost of decrease in relative permittivity. The energy storage calculations showed that the restored energy and efficiency decreased with increasing Na^+ and Nb^{5+} substitution in the host lattice of BNTBT, suggesting that the addition is not useful to enhance its energy storage characteristics.

Asif Ali – PhD, Reseracher;
Hina Zahid – MS, Researcher..

[1] R.H. Havemann, B.E. Gnade, C.-C. Cho, Porous dielectric material with a passivation layer for electronics applications (Google Patents, 1997).
[2] R. Muhammad, Y. Iqbal, I.M. Reaney, J. Am. Ceram. Soc. 99, 2089 (2016); https://doi.org/10.1111/jace.14212.
[3] R. Muhammad, Y. Iqbal, Ceram. Int. 42, 19413 (2016); https://doi.org/10.1016/j.ceramint.2016.08.152.
[4] S.-E. Park, T.R. Shrout, J. Appl. Phys. 82, 1804 (1997); https://doi.org/10.1063/1.365983.
[5] K. Yao, S. Chen, M. Rahimabady, M.S. Mirshekarloo, S. Yu, F.E.H. Tay, T. Sritharan, L. Lu, IEEE Trans. Sonics Ultrason. 58, 1968 (2011); https://doi.org/10.1109/TUFFC.2011.2039.
[6] B. Ma, M. Narayanan, S. Tong, U. Balachandran, J. Mater. Sci. 45, 151 (2010); https://doi.org/10.1007/s10853-009-3910-0.
[7] N. Zhang, L. Li, J. Chen, J. Yu, Mater. Lett. 138, 228 (2015); https://doi.org/10.1016/j.matlet.2014.09.123.
[8] Y. Li, W. Chen, Q. Xu, J. Zhou, X. Gu, Mater. Lett. 59, 1361 (2005); https://doi.org/10.1016/j.matlet.2004.12.041.
[9] V. Shuvaeva, D. Zekria, A. Glazer, Q. Jiang, S. Weber, P. Bhattacharya, P. Thomas, Phys. Rev. B 71, 174114 (2005); https://doi.org/10.1103/PhysRevB.71.174114.
[10] R. Muhammad, A. Khesro, M. Uzair, J. Electron. Mater. 45, 4083 (2016); https://doi.org/10.1007/s11664-016-4589-z.
[11] A. Zeb, S. Milne, J. Mater. Sci.: Mater. Electron. 26, 9243 (2015); https://doi.org/10.1007/s10854-015-3707-7.
V.R. Mudinepalli, N.R. Reddy, W.-C. Lin, K.S. Kumar, B. Murty, Adv. Mater. Lett. 6, 27 (2015); https://doi.org/10.1007/s12648-015-0743-3.
[12] S.T. Zhang, A.B. Kounga, E. Aulbach, Y. Deng, J. Am. Ceram. Soc. 91, 3950 (2008); https://doi.org/10.1111/j.1551-2916.2008.02778.x.
[13] M. Isaza-Ruiz, J. Henon, O. Durand-Panteix, G. Etchegoyen, F. Rossignol, P. Marchet, Ceram. Int. 42, 14635 (2016); https://doi.org/10.1016/j.ceramint.2016.06.084.
X.S. Qiao, X.M. Chen, H.L. Lian, W.T. Chen, J.P. Zhou, P. Liu, J. Am. Ceram. Soc. 99, 198 (2016); https://doi.org/10.1111/jace.13941.
[14] X. Lu, J. Xu, L. Yang, C. Zhou, Y. Zhao, C. Yuan, Q. Li, G. Chen, H. Wang, J. Materiomics 2, 87 (2016); https://doi.org/10.1016/j.jmat.2016.02.001.
[15] F. Gao, X. Dong, C. Mao, H. Zhang, F. Cao, G. Wang, J. Appl. Phys. 110, 094109 (2011); https://doi.org/10.1063/1.3660283.
[16] Q. Xu, H. Liu, Z. Song, X. Huang, A. Ullah, L. Zhang, J. Xie, H. Hao, M. Cao, Z. Yao, J. Mater. Sci.: Mater. Electron. 27, 322 (2016); https://doi.org/10.1007/s10854-015-3757-x.
[17] R. Muhammad, J. Camargo, A. Prado, M.S. Castro, Mater. Lett. 233, 258 (2018); https://doi.org/10.1016/j.matlet.2018.09.022.
[18] R. Muhammad, A. Ali, J. Camargo, M.S. Castro, ChemistrySelect. 5, 3730 (2020); https://doi.org/10.1002/slct.202000243.
[19] Q. Xu, T. Li, H. Hao, S. Zhang, Z. Wang, M. Cao, Z. Yao, H. Liu, J. Eur. Ceram. Soc. 35, 545 (2015); https://doi.org/10.1016/j.jeurceramsoc.2014.09.003.
[20] R.D. Shannon, Acta Crystallogr. A 32, 751 (1976); https://doi.org/10.1107/S0567739476001551.
[21] Q. Xu, Z. Song, W. Tang, H. Hao, L. Zhang, M. Appiah, M. Cao, Z. Yao, Z. He, H. Liu, J. Am. Ceram. Soc. 98, 3119 (2015); https://doi.org/10.1111/jace.13693.
[22] M.K. Niranjan, T. Karthik, S. Asthana, J. Pan, U.V. Waghmare, J. Appl. Phys. 113, 194106 (2013); https://doi.org/10.1063/1.4804940.

[23] J. Hao, B. Shen, J. Zhai, C. Liu, X. Li, X. Gao, J. Appl. Phys. 113, 114106 (2013); https://doi.org/10.1063/1.4795511.
[24] R. Muhammad, A. Khesro, J. Am. Ceram. Soc. 100, 1091 (2017); https://doi.org/10.1111/jace.14684.
[25] D. Tenne, A. Soukiassian, M. Zhu, A. Clark, X. Xi, H. Choosuwan, Q. He, R. Guo, A. Bhalla, Phys. Rev. B 67, 012302 (2003); https://doi.org/10.1103/PhysRevB.67.012302.
[26] R.D. Shannon, J. Appl. Phys. 73, 348 (1993); https://doi.org/10.1063/1.353856.
J. Suchanicz, I. Jankowska-Sumara, T.V. Kruzina, J. Electroceram. 27, 45 (2011); https://doi.org/10.1007/s10832-011-9648-5.
I. Siny, E. Husson, J. Beny, S. Lushnikov, E. Rogacheva, P. Syrnikov, Ferroelectrics 248, 57 (2000); https://doi.org/10.1080/00150190008223669.
[27] M. Zannen, A. Lahmar, M. Dietze, H. Khemakhem, A. Kabadou, M. Es-Souni, Mater. Chem. Phys. 134, 829 (2012); https://doi.org/10.1016/j.matchemphys.2012.03.076.

Асіф Алі, Хайна Захід

Діелектричні, сегнетоелектричні та оптичні властивості $(Bi_{0,5}Na_{0,5})_{0,94}Ba_{0,06}TiO_3$, легованого Na та Nb

Фізичний факультет, Університет Абдул Валі Хана Мардан, Пакистан, asif.lfmd@gmail.com

Керамічний $[(Bi_{0.5}Na_{0.5})_{0.94}Ba_{0.06}]_{1-x}Na_xTi_{1-x}Nb_xO_3$ (x = 0.05 та 0.10) отримано відомим способом твердотільного спікання. Рентгенодифракційний аналіз зразків вказав на формування кубічної структури. Подібна структура спостерігається із раманівських спектрів досліджуваних зразків. Оптична ширина забороненої зони зразків дещо зменшувалася від 3,08 до 3,06 еВ при додаванні рівнів Na^+ та Nb^{5+}. Додавання Na^+ і Nb^{5+} змістило T_m у бік кімнатної температури. Зразок із x = 0,05 мав стабільну відносну проникність $\varepsilon_{r(mid)}$ = 3914 у діапазоні температур 79 - 350 °C і tanδ < 0,025 (104 - 279 °C). Густина енергії зразка із x = 0,05 становила 0,4 Дж/см^3, яка зменшилась до 0,32 Дж/см^3 при накладанні електричного поля 50 кВ/см з подальшим заміщенням Na^+ і Nb^{5+} (тобто x = 0,10).

Ключові слова: $BaTiO_3$; $Bi_{0.5}Na_{0.5}TiO_3$; діелектричні властивості; фероелектричні властивості; густина енергії.